



Competing effects of crustal shortening, thermal inheritance, and surface processes explain subsidence anomalies in inverted rift basins

Éva Oravecz^{1,2,*}, Attila Balázs², Taras Gerya², Dave A. May³, and László Fodor^{1,4}

¹Department of Applied and Physical Geology, Institute of Geography and Earth Sciences, Eötvös Loránd University, Pázmány P. sétány 1/C, 1117 Budapest, Hungary

²Department of Earth Sciences, Institute of Geophysics, ETH Zürich, Sonneggstrasse 5, 8092 Zürich, Switzerland

³Institute of Geophysics and Planetary Physics, Scripps Institution of Oceanography, University of California–San Diego, 9500 Gilman Drive 0202, La Jolla, California 92093, USA

⁴Institute of Earth Physics and Space Science, Csatkai E. u. 6-8, 9400 Sopron, Hungary

ABSTRACT

Structural inversion of rifted basins is generally associated with surface uplift and denudation of the sedimentary infill, reflecting the active contractional deformation in the crust. However, worldwide examples of inverted rifts show contrasting basin-scale subsidence and widespread sedimentation patterns during basin inversion. By conducting a series of three-dimensional coupled geodynamic and surface processes models, we investigated the dynamic controls on these subsidence anomalies during the successive stages of rifting and basin inversion, and we propose a new evolutionary model for this process. Our models show that the inherited thermo-rheological properties of the lithosphere influence the initial strain localization and subsequent migration of crustal deformation during inversion. The sense of the vertical movements (i.e., uplift or subsidence), however, is not directly linked to the underlying crustal stress patterns; rather, it reflects the balance among contraction-induced tectonic uplift, postrift thermal subsidence of the inherited lithosphere, and sediment redistribution. Based on the interplay among the competing differential vertical movements with different amplitudes and wavelengths, inversion of rifted basins may lead to the growth of intraplate orogens, or the contraction-driven localized uplift may be hindered by the thermal sag effects of the inherited shallow lithosphere–asthenosphere boundary, resulting in basin-scale subsidence. In such basins, dating the first erosional surfaces and other unconformities may not provide accurate timing for the onset of inversion.

INTRODUCTION

Structural inversion of rifted basins is a result of the governing plate motion change from divergence to convergence, which corresponds to the end of rifting and initiation of contractional deformation in the inherited rift system (Cooper et al., 1989; Turner and Williams, 2004). On a crustal scale, the resulting basin inversion in fossil continental rifts is characterized by the diachronous reactivation of the existing extensional structures and/or formation of new contractional structures, which is generally associated with surface uplift and

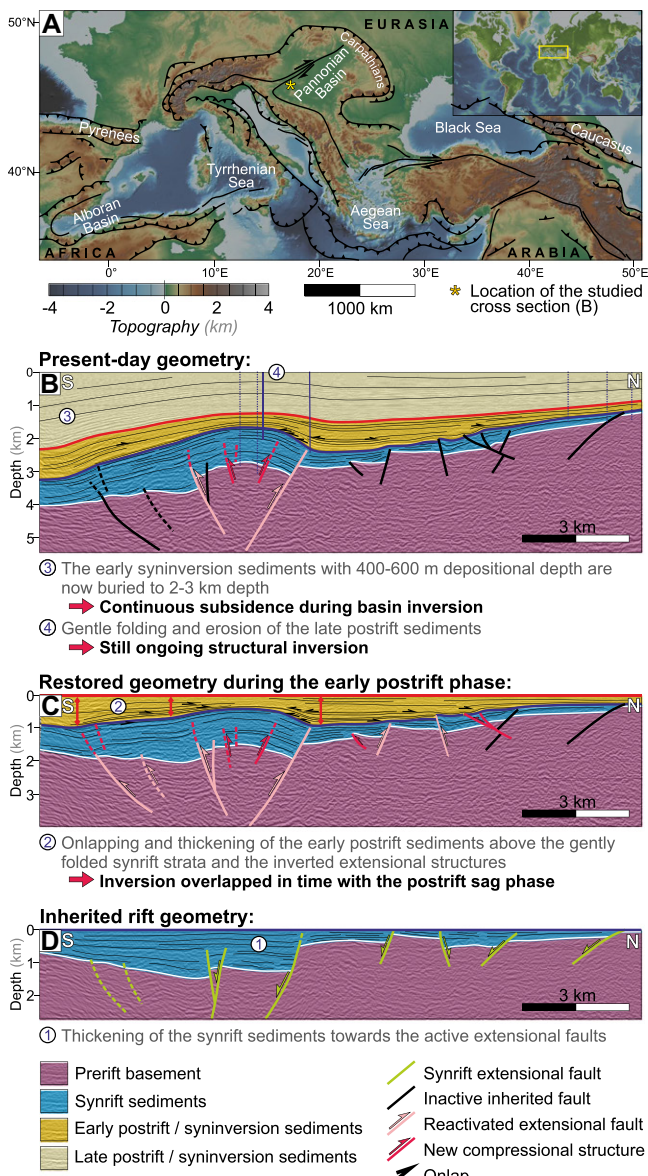
sediment redistribution from the exhuming depocenters toward the margins (Stüwe and Barr, 1998; Zwaan et al., 2022), ultimately leading to the development of intraplate orogens. However, instead of uplift and erosion, many inverted rift basins worldwide show counterintuitive basin-scale subsidence during inversion. Examples include the Permian Basin in west Texas (Fairhurst et al., 2021), Gulf of Mexico (Roure et al., 2009), South China Sea (Xie et al., 2017), Aquitaine Basin (Angrand et al., 2018; Dielforder et al., 2019), Tyrrhenian Sea (Zitellini et al., 2020), and Pannonian Basin (Fig. 1A; Horváth and Cloetingh, 1996). In the latter, the change from back-arc rifting to basin inversion occurred within a short (~2 m.y.) interval, when slab rollback along the Carpathian subduction

zone ceased (Horváth et al., 2015), and the slow-rate (1–2 mm/yr) northward convergence of the Adriatic plate became dominant (Fodor et al., 2005; Bada et al., 2007). While traditional tectonic models discretely separate the synrift, postrift, and inversion phases and correlate the onset of inversion with the onset of uplift and formation of erosional unconformities, seismic profiles from the SW Pannonian Basin show that even the earliest postrift deposition was coeval with the structural inversion of the underlying synrift structures, implying significant temporal overlap between the postrift sag and inversion phases (Figs. 1B–1D; Tari et al., 2020). Compared to the ~600 m depositional paleobathymetry (Balázs et al., 2018), the subsequent burial of these early postrift sediments implies continuous subsidence despite the coeval structural inversion.

These anomalous subsidence patterns in inverted rifts indicate an important coupling among the changing stress field, thermal evolution of the lithosphere, differential vertical movements, and sedimentation, which is yet to be understood. While the uplift rates are predominantly controlled by variable convergence rates, the tectonic evolution of the forming orogens is also influenced by inherited rheological properties of the lithosphere (Jammes and Huismans, 2012), preexisting structural heterogeneities (Ruh and Vergés, 2018; Granda and Ruh, 2019), and syntectonic surface processes (Willett, 1999; Whipple and Meade, 2004; Erdős et al., 2014). The thermal state of the lithosphere, in particular, has been recognized to control strain localization via thermal weakening (Jourdon et al., 2019) and affect the

Éva Oravecz  <https://orcid.org/0000-0003-1032-1564>
*orav.eva@gmail.com

CITATION: Oravecz, É., et al., 2024, Competing effects of crustal shortening, thermal inheritance, and surface processes explain subsidence anomalies in inverted rift basins: *Geology*, v. 52, p. 447–452, <https://doi.org/10.1130/G51971.1>



style of inversion by controlling lithospheric strength (Buiter et al., 2009); however, its role in the surface evolution during inversion has remained unexplored.

In this work, we investigated the physical controls on contrasting subsidence anomalies during rift inversion by using three-dimensional (3-D) lithospheric-scale geomorphologic-geodynamic numerical models. The applied two-way coupling between the thermo-mechanical and surface processes models allowed for dynamic feedback mechanisms among crustal tectonics, thermal evolution, melting, erosion/sedimentation, and topographic evolution. Our simulations, in agreement with inferences from the Pannonian Basin, also involved the preceding rifting stage to account for structural and thermal inheritance. The models documented strain patterns and differential vertical movements that varied in space and time during basin inversion, reflecting the dynamic interplay

among the convergence rates, inherited thermo-rheological structure of the lithosphere, and the rate of diffusion-driven surface processes.

NUMERICAL SETUP

We used the I3ELVIS magmatic-thermo-mechanical code coupled to the FDSPM surface processes code to simulate rifting and subsequent basin inversion (Gerya, 2013; Munch et al., 2022). The code employs visco-plastic rheologies and includes grain-size evolution, plastic weakening, and simplified magma-related processes, such as partial melting and melt extraction (see the Supplemental Material).¹ Our initial

model setup included a layered lithosphere with a thick orogenic-type crust and mantle above the asthenosphere (Fig. S1). A hydrated weak zone was defined in the mantle lithosphere that represents a suture zone inherited from a previous subduction and collision stage of the Wilson cycle. This zone was oriented oblique to the imposed velocity field in order to better approximate natural observations of oblique rifts worldwide (Brune et al., 2018), including the Pannonian Basin (Csontos and Nagymarosy, 1998; Fodor et al., 2021). Two end-member models were compared in detail to show the contrasting effects of different convergence velocities during inversion. In both cases, rifting was simulated for 8 m.y. by imposing a constant 2 cm/yr divergent velocity, equally divided between the two model sides. Subsequent basin inversion was simulated by switching the boundary condition to a constant 2 cm/yr or 2 mm/yr convergent velocity. Further model results showing the effects of other divergence/convergence velocities and the rates of surface processes, as well as discussion of the model limitations, are shown in the Supplemental Material.

NUMERICAL MODEL EVOLUTION Continental Rifting

Rift initiation corresponds to the reactivation of the inherited suture zone and development of the first depocenter in the upper crust (Fig. 2A; Dep. 1 in Fig. 3). The crustal deformation migrates in space, successively forming new depocenters, first at the future margins of the rift (Dep. 2) and then toward the basin center (Dep. 3) as active faulting gradually ceases at the margins. The active synrift depocenters show ~4 m.y. of fast-rate (1–6 mm/yr) hanging-wall subsidence and footwall uplift, followed by tectonic quiescence or even slow-rate (~0.2 mm/yr) uplift as deformation relocates in the subsequent younger synrift subbasin. Lithospheric thinning governs the gradually increasing temperature values, which result in lower-crustal partial melting from 6.4 m.y. on, followed by decompressional mantle melting from 8.1 m.y. on. By the end of the synrift phase, a continental rift system has developed, floored by ~20 km of crust and 30 km of mantle lithosphere.

Structural Inversion of Rifted Basins

The reversal from divergent to convergent velocities marks the onset of basin inversion. Initial contractional strain localization occurs in the basin center, which is rheologically the weakest part of the lithosphere due to the inherited shallow lithosphere–asthenosphere boundary (LAB) and related thermal and melt-induced weakening (Figs. 2B and 2C). The first surface response to the onset of inversion is the slow-rate (0.1–0.4 mm/yr) uplift of the basin center and the subsidence of the rift margins in both models (Dep. 3 in Figs. 3A and 3B).

¹Supplemental Material. Details of the applied numerical methods, model configurations, and additional model results. Please visit <https://doi.org/10.1130/GEOL.S.25308742> to access the supplemental material; contact editing@geosociety.org with any questions.

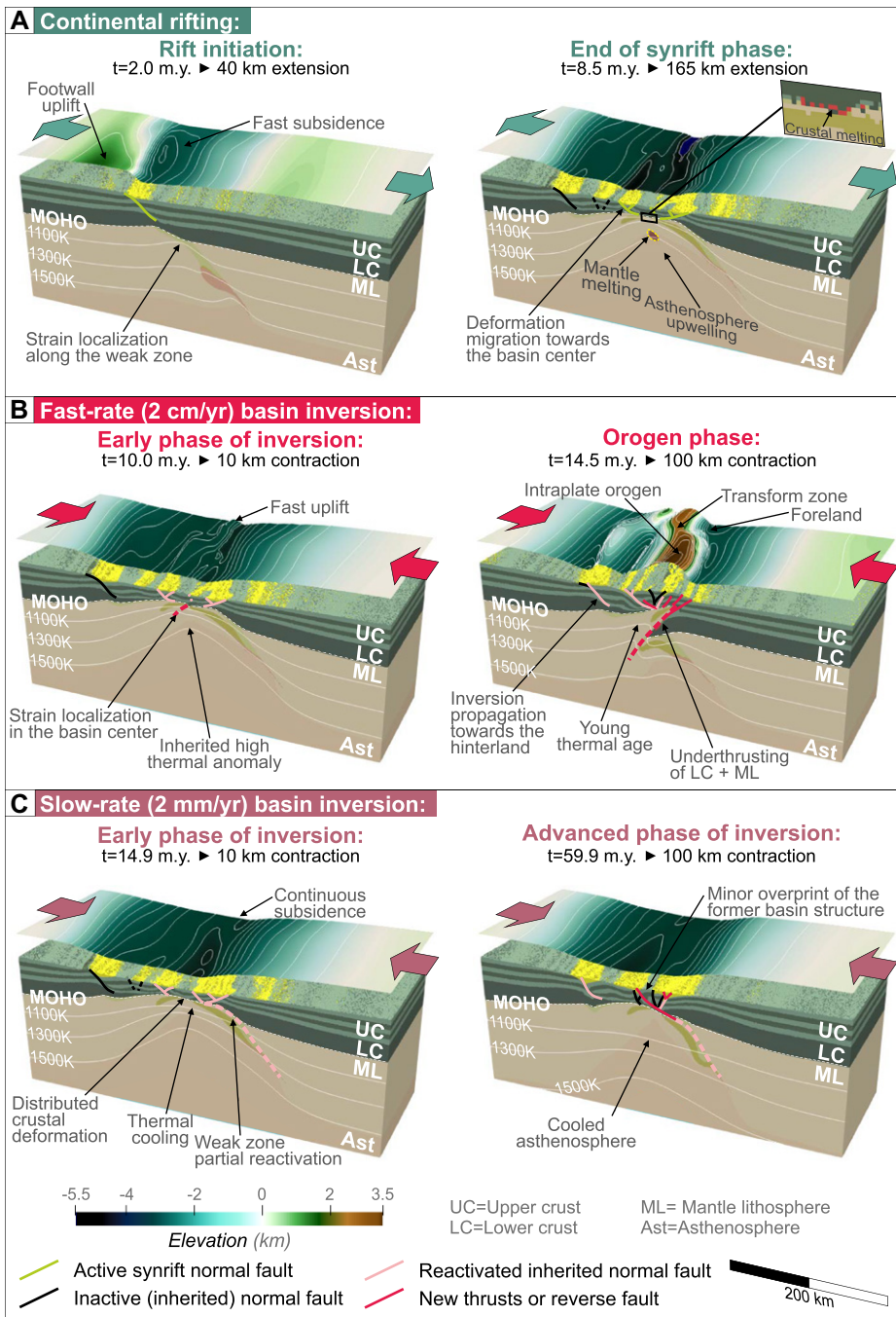


Figure 2. Numerical model evolution of continental rifting and subsequent basin inversion. (A) Rift initiation and late-stage synrift structure, with thermally weakened and thinned lithosphere. (B) Fast-rate (2 cm/yr) basin inversion. Underthrusting of lower crust below upper crust initiates at rheologically weakest part of inherited lithosphere and leads to uplift of basin center and subsidence of foreland margins. (C) Slow-rate (2 mm/yr) basin inversion. Thermal subsidence rate of inherited lithosphere–asthenosphere boundary exceeds contraction-driven uplift rate, leading to subsidence and basin-scale sedimentation.

When the convergence is fast, deformation in the weak lithosphere triggers underthrusting of the lower crust beneath the basin center (Fig. 2B). However, with low-rate convergence, to reach the same amount of shortening, the LAB is affected by more thermal cooling, which results in a colder and stronger lithosphere and leads to the relocalization

of deformation along the inherited weak zone (Fig. 2C). In both cases, crustal shortening is first accommodated by contractional reactivation of the inherited extensional fault zones overlying the weak mantle, followed by the gradual migration of deformation toward the older depocenters in the basin margins. Following further shortening, in-sequence thrusting

dominates the foreland during fast convergence (Fig. 3A). In this case, the vertical motions follow the ongoing crustal deformation patterns, including 1–5 mm/yr uplift of the hanging wall of active reverse faults and 1–2 mm/yr subsidence in their footwalls (Fig. 3C). In contrast, the slow convergence model shows more distributed crustal strain patterns with prolonged reactivation of the inherited extensional structures. More importantly, the slowly inverting depocenters undergo continuous basin-scale subsidence (0.05–0.2 mm/yr), which is driven by the thermal cooling of the lithosphere (Figs. 3B and 3C). Upon reaching 100 km of convergence, fast convergence results in the development of an asymmetric, thick-skinned intraplate orogenic wedge, characterized by strong structural overprint on the former rift structure, whereas thermal subsidence is more dominant with slow (low-rate) convergence, creating more accommodation space and enhancing the role of postrift sedimentation.

GEOLOGICAL IMPLICATIONS

Our models explain two important aspects of rift inversion. First, strain is localized at different depocenters at different times; therefore, the onset of structural inversion is diachronous across the rift system, and the different depocenters show strikingly different subsidence histories (Fig. 3C). Because the transition from rifting to inversion is short, initial strain localization occurs in the basin center instead of the margins, controlled by the inherited thermal and melt-induced weakening, while the subsequent spatial migration of deformation is linked to the shortening rate and the thermo-rheological state of the lithosphere (Figs. 3A and 3B).

Second, structural inversion of rifted basins is associated with either uplift or subsidence, controlled by the competing effects of several superimposed processes with different wavelengths and amplitudes. While crustal shortening governs the short-wavelength ($\lambda \sim 10$ km) vertical motions that are linked to the stress field in the crust, the postrift thermal cooling and the spatial distribution of sediments impose a longer-wavelength ($\lambda \sim 100$ km) sag subsidence on the lithosphere (Fig. 4A). The contraction-driven tectonic uplift rates are primarily governed by the rate of convergence, whereas the postrift thermal subsidence is linked to the feedback mechanisms among rift kinematics, thermal evolution, and surface processes. The inherited 3-D thermal structure is connected to the initial lithospheric structure and the rate and duration of rifting (cf. Cacace and Scheck-Wenderoth, 2016; Balázs et al., 2021), and it strongly affects the postrift thermal subsidence rates (Figs. S7, S8, and S10A). Along with the intensity of surface processes, this factor determines the spatial and temporal distribution of sediments, which in turn influences strain localization, sediment loading, and

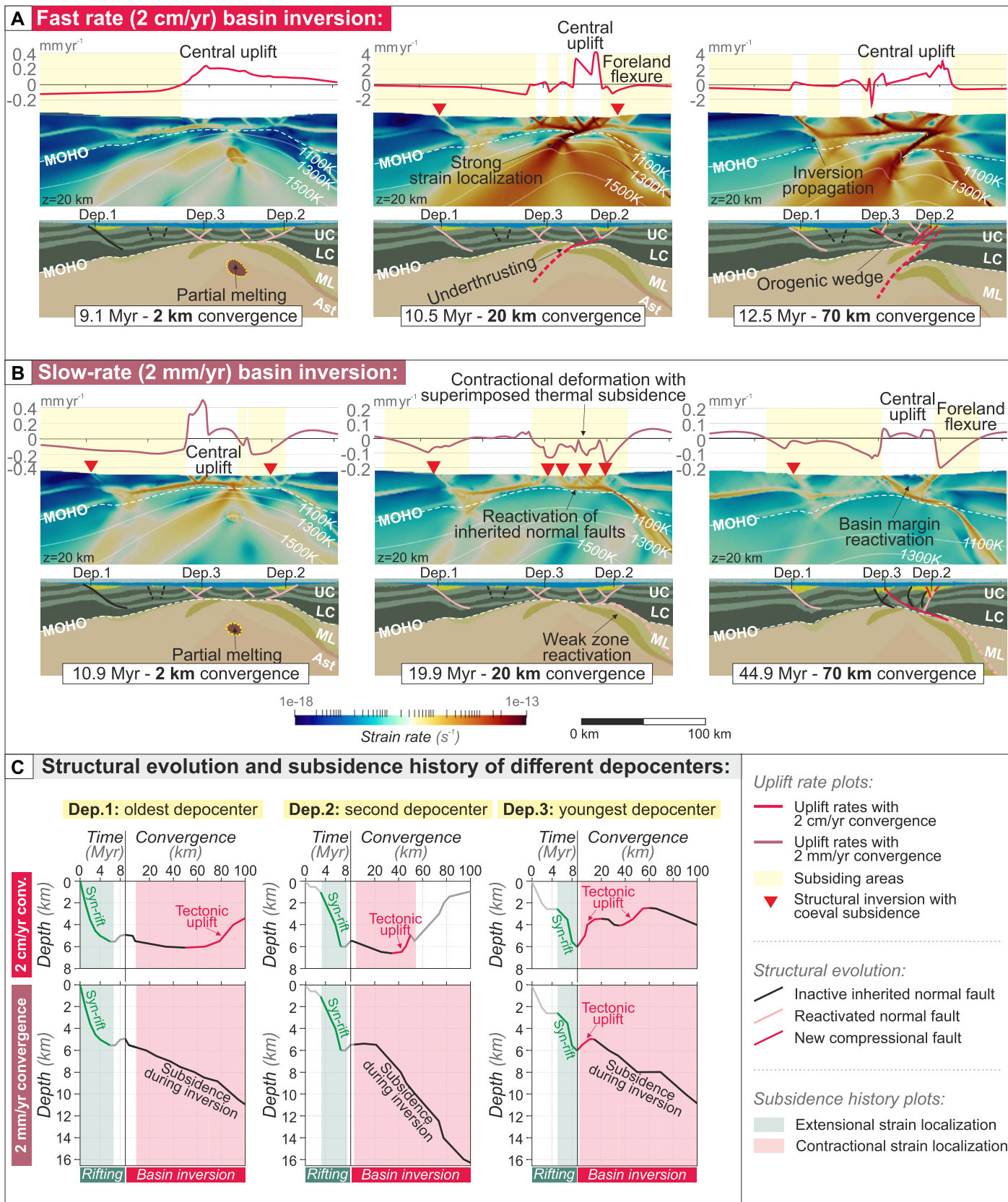
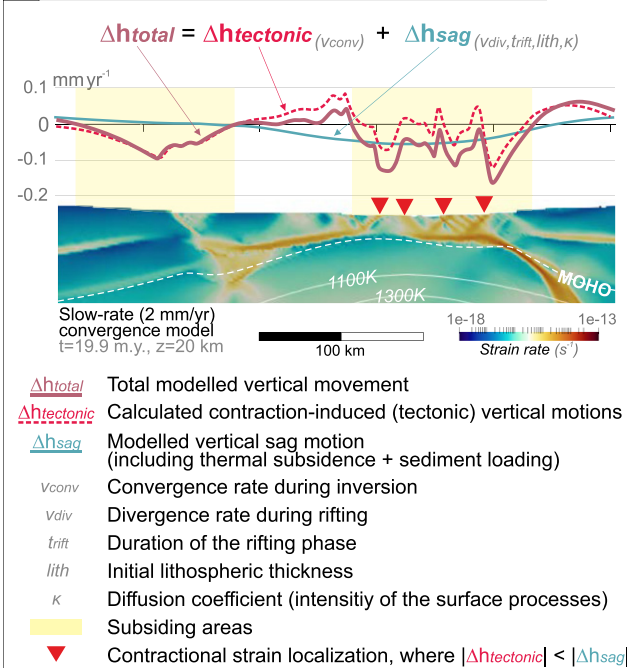
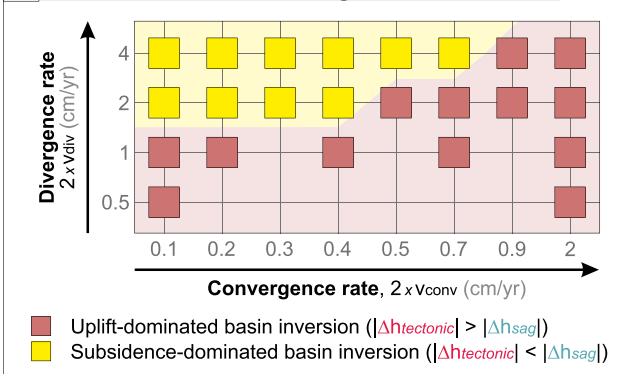


Figure 3. Spatial and temporal variations of crustal strain patterns and differential vertical movements. (A–B) Basin structure, strain rate evolution, and surface uplift rates along same sections from fast-rate (2 cm/yr) and slow-rate (2 mm/yr) inversion models, after same amount of convergence. Red triangles mark actively deforming, yet constantly subsiding structures that are linked to thermal cooling of mantle. UC—upper crust; LC—lower crust; ML—mantle lithosphere; Ast—asthenosphere. (C) Subsidence history of three depocenters, showing depth of sediment–basement interface. Plots highlight diachronous onset of structural inversion across basin and show that there is no direct link between sense of vertical movements and underlying crustal stress patterns.

A Components of the vertical movements:



B How effective is Δh_{sag} against $\Delta h_{tectonic}$?



the thermal blanketing (Figs. S9 and S10B; cf., Burov and Cloetingh, 1997; Olive et al., 2014; Wolf et al., 2021).

These results show that the sense of vertical movements is not directly linked to the underlying crustal stress patterns. Instead, the modeled surface motions reflect the relations among tectonic uplift, thermal subsidence, and the rate of sedimentation. At low convergence rates, the postrift sag may outpace the tectonic uplift, and the early phase of inversion is governed by subsidence. The threshold convergence rate, which determines whether the inversion is linked to uplift or subsidence, depends on the inherited temperature field (Fig. 4B) and the duration of tectonic quiescence between the synrift and inversion phases. The initial synconvergence subsidence is eventually switched to uplift-dominated evolution when the contraction-driven vertical motions finally outpace the effect of thermal relaxation.

Our models demonstrate that since the early surface response of basin inversion can be subsidence, dating the first erosional surfaces and unconformities in inverted rifts and orogens may not provide accurate timing for the reversal from divergence to convergence. This may be the case when the inversion significantly overlaps in time with the postrift sag phase, which is a particularly viable scenario in tectonic settings characterized by fast changes in the stress field, for instance, in back-arc basins, including the Pannonian Basin (Fig. 1).

CONCLUSIONS

Our 3-D coupled thermo-mechanical and surface processes models explain new aspects of inverted rift systems:

1. The crustal stress patterns do not directly indicate whether surface uplift or subsidence occurred during inversion. Instead, the observed vertical motions reflect the relations among convergence rate, postrift thermal subsidence, and

sediment redistribution. Therefore, when the inversion significantly overlaps in time with the postrift sag phase, the sag subsidence resulting from the inherited mantle conditions may outpace the tectonic uplift at low convergence rates, leading to basin-scale subsidence and increased sedimentary burial during inversion. This has implications for interpreting regional unconformities as the primary signs of inversion initiation.

2. In inverting young rifts, localization of the first inverted structures occurs in the basin center instead of the margins, controlled by the inherited thermo-rheological properties of the lithosphere, while subsequent migration of deformation is mainly linked to the shortening rate, thermo-rheological state of the lithosphere, and inherited extensional structures.

ACKNOWLEDGMENTS

The constructive reviews by Anthony Jourdon, Frank Zwaan, two anonymous reviewers, and editor Rob Strachan are acknowledged. A. Balázs and T. Gerya acknowledge support from Swiss National Science Foundation Research Grant 200021_192296 and from International Lithosphere Program Task Force "Bio-Geodynamics of the Lithosphere." D. May acknowledges support from National Science Foundation grant EAR-2121568, and L. Fodor acknowledges support from the Hungarian National Innovation Office (NKFIH) OTKA 134873 fund. All computations were performed on the ETH Zürich Euler Cluster.

REFERENCES CITED

- Angrald, P., Ford, M., and Watts, A.B., 2018, Lateral variations in foreland flexure of a rifted continental margin: The Aquitaine Basin (SW France): *Tectonics*, v. 37, p. 430–449, <https://doi.org/10.1029/2017TC004670>.
- Bada, G., Horváth, F., Dövényi, P., Szafián, P., Windhoffer, G., and Cloetingh, S., 2007, Present-day stress field and tectonic inversion in the Pannonian Basin: *Global and Planetary Change*, v. 58, p. 165–180, <https://doi.org/10.1016/j.gloplacha.2007.01.007>.
- Balázs, A., Magyar, I., Matenco, L., Sztanó, O., Tókés, L., and Horváth, F., 2018, Morphology of a large paleo-lake: Analysis of compaction in the Miocene–Quaternary Pannonian Basin: *Global and Planetary Change*, v. 171, p. 134–147, <https://doi.org/10.1016/j.gloplacha.2017.10.012>.
- Balázs, A., Matenco, L., Granjeon, D., Alms, K., François, T., and Sztanó, O., 2021, Towards stratigraphic-thermo-mechanical numerical modelling: Integrated analysis of asymmetric extensional basins: *Global and Planetary Change*, v. 196, <https://doi.org/10.1016/j.gloplacha.2020.103386>.
- Brune, S., Williams, S.E., and Müller, R.D., 2018, Oblique rifting: The rule, not the exception: *Solid Earth*, v. 9, p. 1187–1206, <https://doi.org/10.5194/se-9-1187-2018>.
- Buiter, S.J.H., Pfiffner, O.A., and Beaumont, C., 2009, Inversion of extensional sedimentary basins: A numerical evaluation of the localization of shortening: *Earth and Planetary Science Letters*, v. 288, p. 492–504, <https://doi.org/10.1016/j.epsl.2009.10.011>.
- Burov, E., and Cloetingh, S., 1997, Erosion and rift dynamics: New thermomechanical aspects of post-rift evolution of extensional basins: *Earth and Planetary Science Letters*,

v. 150, p. 7–26, [https://doi.org/10.1016/S0012-821X\(97\)00069-1](https://doi.org/10.1016/S0012-821X(97)00069-1).

Cacace, M., and Scheck-Wenderoth, M., 2016, Why intracontinental basins subside longer: 3-D feedback effects of lithospheric cooling and sedimentation on the flexural strength of the lithosphere: *Journal of Geophysical Research: Solid Earth*, v. 121, p. 3742–3761, <https://doi.org/10.1002/2015JB012682>.

Cooper, M.A., Williams, G.D., de Graciansky, P.C., Murphy, R.W., Needham, T., de Paor, D., Stonerley, R., Todd, S.P., Turner, J.P., and Ziegler, P.A., 1989, Inversion tectonics—A discussion, in Cooper, M.A., and Williams, G.D., eds., *Inversion Tectonics*: Geological Society, London, Special Publication 44, p. 335–347, <https://doi.org/10.1144/GSL.SP.1989.044.18.18>.

Csontos, L., and Nagymarosy, A., 1998, The Mid-Hungarian line: A zone of repeated tectonic inversions: *Tectonophysics*, v. 297, p. 51–71, [https://doi.org/10.1016/S0040-1951\(98\)00163-2](https://doi.org/10.1016/S0040-1951(98)00163-2).

Dielforder, A., Frasca, G., Brune, S., and Ford, M., 2019, Formation of the Iberian-European convergent plate boundary fault and its effect on intraplate deformation in central Europe: *Geochemistry, Geophysics, Geosystems*, v. 20, p. 2395–2417, <https://doi.org/10.1029/2018GC007840>.

Erdős, Z., Huismans, R.S., van der Beek, P., and Thieulot, C., 2014, Extensional inheritance and surface processes as controlling factors of mountain belt structure: *Solid Earth*, v. 119, p. 9042–9061, <https://doi.org/10.1002/2014JB011408>.

Faccenna, C., Becker, T.W., Auer, L., Billi, A., Boschi, L., Brun, J.P., Capitanio, F.A., Funiciello, F., Horváth, F., Jolivet, L., Piromallo, C., Royden, L., Rossetti, F., and Serpelloni, E., 2014, Mantle dynamics in the Mediterranean: Reviews of Geophysics, v. 52, p. 283–332, <https://doi.org/10.1002/2013RG000444>.

Fairhurst, B., Ewing, T., and Lindsay, B., 2021, West Texan (Permian) Super Basin, United States: Tectonics, structural development, sedimentation, petroleum systems, and hydrocarbon reserves: *American Association of Petroleum Geologists Bulletin*, v. 105, p. 1099–1147, <https://doi.org/10.1306/03042120130>.

Fodor, L., Bada, G., Csillag, G., Horváth, E., Ruszkicay-Rüdiger, Zs., Palotás, K., Síkhegyi, F., Timár, G., Cloetingh, S., and Horváth, F., 2005, An outline of neotectonic structures and morphotectonics of the western and central Pannonian Basin: *Tectonophysics*, v. 410, p. 15–41, <https://doi.org/10.1016/j.tecto.2005.06.008>.

Fodor, L., Balázsová, A., Csillag, G., Dunkl, I., Héja, G., Jelen, B., Kelemen, P., Kovér, Sz., Németh, A., Nyíri, D., Selmeczi, I., Trajanova, M., Vrabec, M., and Vrabec, M., 2021, Crustal exhumation and depocenter migration from the Alpine orogenic margin towards the Pannonian extensional back-arc basin controlled by inheritance: *Global and Planetary Change*, v. 201, <https://doi.org/10.1016/j.gloplacha.2021.103475>.

Gerya, T.V., 2013, Initiation of transform faults at rifted continental margins: 3D petrological-thermomechanical modeling and comparison to the Woodlark Basin: *Petrology*, v. 21, p. 550–560, <https://doi.org/10.1134/S0869591113060039>.

Granado, P., and Ruh, J.B., 2019, Numerical modeling of inversion tectonics in fold-and-thrust belts: *Tectonophysics*, v. 763, p. 14–29, <https://doi.org/10.1016/j.tecto.2019.04.033>.

Horváth, F., and Cloetingh, S., 1996, Stress-induced late-stage subsidence anomalies in the Pannonian Basin: *Tectonophysics*, v. 266, p. 287–300, [https://doi.org/10.1016/S0040-1951\(96\)00194-1](https://doi.org/10.1016/S0040-1951(96)00194-1).

Horváth, F., Musitz, B., Balázsová, A., Végh, A., Uhrin, A., Nádor, B., Koroknai, B., Pap, N., Tóth, T., and Wórum, G., 2015, Evolution of the Pannonian Basin and its geothermal resources: *Geothermics*, v. 53, p. 328–352, <https://doi.org/10.1016/j.geothermics.2014.07.009>.

Jammes, S., and Huismans, R.S., 2012, Structural styles of mountain building: Controls of lithospheric rheological stratification and extensional inheritance: *Journal of Geophysical Research*, v. 117, B10403, <https://doi.org/10.1029/2012JB009376>.

Jourdon, A., Le Pourhiet, L., Mouthereau, F., and Masiá, E., 2019, Role of rift maturity on the architecture and shortening distribution in mountain belts: *Earth and Planetary Science Letters*, v. 512, p. 89–99, <https://doi.org/10.1016/j.epsl.2019.01.057>.

Munch, J., Ueda, K., Schnydrig, S., May, D.A., and Gerya, T.V., 2022, Contrasting influence of sediments vs. surface processes on retreating subduction zones dynamics: *Tectonophysics*, v. 836, <https://doi.org/10.1016/j.tecto.2022.229410>.

Olive, J.-A., Behn, M.D., and Malatesta, L.C., 2014, Modes of extensional faulting controlled by surface processes: *Geophysical Research Letters*, v. 41, p. 6725–6733, <https://doi.org/10.1002/2014GL061507>.

Roure, F., Alzaga-Ruiz, H., Callot, J.-P., Ferket, H., Granjeon, D., Gonzalez-Mercado, G.E., Guilhau-mou, N., Lopez, M., Mougin, P., Ortuno-Arzate, S., and Séranne, M., 2009, Long lasting interactions between tectonic loading, unroofing, post-rift thermal subsidence and sedimentary transfers along the western margin of the Gulf of Mexico: Some insights from integrated quantitative studies: *Tectonophysics*, v. 475, p. 169–189, <https://doi.org/10.1016/j.tecto.2009.04.012>.

Ruh, J.B., and Vergés, J., 2018, Effects of reactivated extensional basement faults on structural evolution of fold-and-thrust belts: Insights from numerical modelling applied to the Kopet Dagh Mountains: *Tectonophysics*, v. 746, p. 493–511, <https://doi.org/10.1016/j.tecto.2017.05.020>.

Stüwe, K., and Barr, T.D., 1998, On uplift and exhumation during convergence: *Tectonics*, v. 17, p. 80–88, <https://doi.org/10.1029/97TC02557>.

Tari, G., Arbouille, D., Schléder, Zs., and Tóth, T., 2020, Inversion tectonics: A brief petroleum industry perspective: *Solid Earth*, v. 11, p. 1865–1889, <https://doi.org/10.5194/se-11-1865-2020>.

Turner, J.P., and Williams, G.A., 2004, Sedimentary basin inversion and intra-plate shortening: *Earth-Science Reviews*, v. 65, p. 277–304, <https://doi.org/10.1016/j.earscirev.2003.10.002>.

Whipple, K.X., and Meade, B., 2004, Controls on the strength of coupling among climate, erosion, and deformation in two-sided, frictional orogenic wedges at steady state: *Journal of Geophysical Research*, v. 109, F10111, <https://doi.org/10.1029/2003JF000019>.

Willett, S.D., 1999, Orogeny and orography: The effects of erosion on the structure of mountain belts: *Journal of Geophysical Research: Solid Earth*, v. 104, p. 28,957–28,981, <https://doi.org/10.1029/1999JB900248>.

Wolf, S.G., Huismans, R.S., Muñoz, J.-P., Curry, M.E., and van der Beek, P., 2021, Growth of collisional orogens from small and cold to large and hot—Inferences from geodynamic models: *Journal of Geophysical Research: Solid Earth*, v. 126, <https://doi.org/10.1029/2020JB021168>.

Xie, Z., Sun, L., Pang, X., Zheng, J., and Sun, Z., 2017, Origin of the Dongsha event in the South China Sea: *Marine Geophysical Researches*, v. 38, p. 357–371, <https://doi.org/10.1007/s11001-017-9321-8>.

Zitellini, N., Ranero, C.G., Loreto, M.F., Ligi, M., Pastore, M., D’Oriano, F., Sallares, V., Grevenmeyer, I., Moeller, S., and Prada, M., 2020, Recent inversion of the Tyrrhenian Basin: *Geology*, v. 48, p. 123–127, <https://doi.org/10.1130/G46774.1>.

Zwaan, F., Schreurs, G., Buitier, S.J.H., Ferrer, O., Reitano, R., Rudolf, M., and Willingshofer, E., 2022, Analogue modelling of basin inversion: A review and future perspectives: *Solid Earth*, v. 13, p. 1859–1905, <https://doi.org/10.5194/se-13-1859-2022>.

Printed in the USA